



## DESIGN OF VIBRATION ABSORBER USING SPRING AND RUBBER FOR ARMORED VEHICLE 5.56 MM CALIBER RIFLE

Aditya Sukma Nugraha<sup>a,\*</sup>, Bagus Budiwantoro<sup>b</sup>, Estiko Rijanto<sup>a</sup>

<sup>a</sup>Research Center for Electrical Power and Mechatronics, Indonesian Institute of Sciences  
Komplek LIPI Jl. Sangkuriang, Bandung, 40135, Indonesia

<sup>b</sup>Faculty of Mechanical and Aerospace Engineering, Institut Teknologi Bandung  
JL.Ganesha 10, Bandung 40132, Indonesia

Received 24 September 2014; received in revised form 30 October 2014; accepted 30 October 2014  
Published online 24 December 2014

### Abstract

This paper presents a design of vibration absorber using spring and rubber for armored vehicle 5.56 mm caliber rifle. Such a rifle is used in a Remote-Controlled Weapon System (RCWS) or a turret where it is fixed using a two degree of freedom pan-tilt mechanism. A half car lumped mass dynamic model of armored vehicles was derived. Numerical simulation was conducted using fourth order Runge Kutta method. Various types of vibration absorbers using spring and rubber with different configurations are installed in the elevation element. Vibration effects on horizontal direction, vertical direction and angular deviation of the elevation element was investigated. Three modes of fire were applied i.e. single fire, semi-automatic fire and automatic fire. From simulation results, it was concluded that the parallel configuration of damping rubber type 3, which has stiffness of 980,356.04 (N/m<sup>2</sup>) and damping coefficient of 107.37 (N.s/m), and Carbon steel spring whose stiffness coefficient is  $5.547 \times 10^6$  (N/m<sup>2</sup>) provides the best vibration absorption.

Keywords: vibration absorber, spring, rubber, armored vehicle, rifle.

### 1. INTRODUCTION

Turret and RCWS play important role in modern security and defense instruments. They are composed of four main components i.e. rifle, mechanism, sensing and controller. The rifle is fixed using a two degree of freedom pan-tilt mechanism. Its shooting direction should be stabilized against external disturbance. Kinematics stabilization of a pan-tilt mechanism has been reported [1]. Effectiveness of stabilization methods using inverse angle and Inertia Measurement Unit (IMU) has also been investigated [2, 3]. SIFT and SURF methods can be used for object recognition system in a turret or RCWS [4]. Such a turret or RCWS may be installed in a mobile robot for special missions [5, 6].

Experiment has been carried out to identify precision tolerance as a function of distance of a weapon system as shown in Figure 1 [7]. In order to improve precision of the weapon system, modern automotive technology adopts two

vibration attenuation approaches i.e. passive and active [8, 9].

This paper aims to improve vibration attenuation and shock absorption performance of a 5.56 mm caliber rifle armored vehicle fixed with two degree of freedom pan-tilt mechanism using passive approach. A dynamic model of armored vehicle is derived using half car lumped

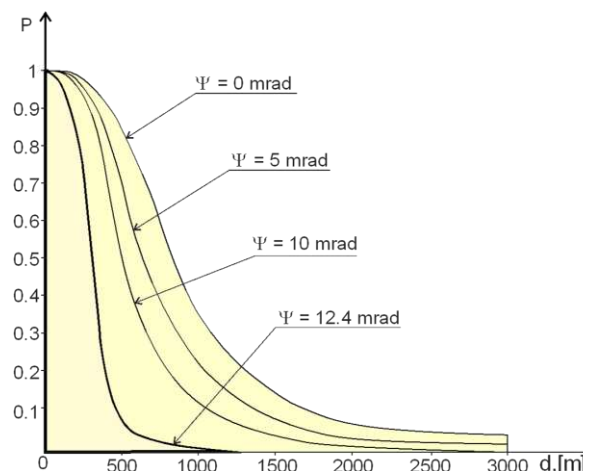


Figure 1. Angle deviation tolerance as a function of distance [7]

\* Corresponding Author: Tel: +62-22-2503055

E-mail: adit003@lipi.go.id

Table 1.  
Numerical parameter of fourth order Runge Kutta [15]

t	x	y	a
$T1 = t_i$	$X1 = x_i$	$Y1 = y_i$	$a1 = a(T_1, X_1, Y_1)$
$T2 = t_i + \frac{\Delta t}{2}$	$X2 = x_i + y1 \frac{\Delta t}{2}$	$Y2 = y_i + a1 \frac{\Delta t}{2}$	$a2 = a(T_2, X_2, Y_2)$
$T3 = t_i + \frac{\Delta t}{2}$	$X3 = x_i + y2 \frac{\Delta t}{2}$	$Y3 = y_i + a2 \frac{\Delta t}{2}$	$A3 = a(T_3, X_3, Y_3)$
$T4 = t_i + \Delta t$	$X4 = x_i + y3 \Delta t$	$Y4 = y_i + a3 \Delta t$	$a4 = a(T_4, X_4, Y_4)$

mass approach [10-14]. Parameter values of the dynamic model are determined based on mechanical characteristics [15-18].

Fourth order Runge Kutta method has been used to solve the dynamic model [19,20]. Numerical parameters used in the Runge Kutta method can be seen in Table 1 [21].

## II. METHODOLOGY

When a turret or RCWS is attached on a vehicle, the structure of the armored vehicle can be illustrated in Figure 2. It consists of elevation component, azimuth component, platform, tires, and road.  $X_e(m)$  and  $Y_e(m)$  represent horizontal and vertical displacements of the elevation component. The rifle shooting angle is determined directly by the elevation component and the azimuth component using an appropriate control system. Irregularity of the road generates external disturbance which should be compensated using stabilization method. Characteristics of the tire and the platform also contribute to the performance of the system.

It is assumed that the armored vehicle is symmetric. A half car lump mass model as shown in Figure 3 is used to simplify the analysis of dynamical model of the armored vehicle.  $K_{ex}(N/m)$  and  $K_{ey}(N/m)$  denote horizontal and vertical stiffness coefficients of the elevation component while  $K_{a1}(N/m)$  and  $K_{a2}(N/m)$  are

the azimuth component stiffness.  $K_{b1}$ ,  $K_{b2}$ ,  $K_{b3}$  and  $K_{b4}$  are the stiffness of the suspension at each tire, respectively.  $K_i(N/m)$  and  $C_i(N.s/m)$  represent stiffness coefficient and damping coefficient of each tire ( $i = 1,2,3,4$ ).

The elevation component has three degrees of freedom including horizontal dislocation, vertical dislocation and elevation angle (pitch). The azimuth component has two degrees of freedom including vertical dislocation and azimuth angle (yaw). The platform has 6 degrees of freedom including vertical dislocation and bouncing of the center of gravity of the platform as well as vertical dislocation of each tire. Thus, the overall model has 11 degrees of freedom.

Motion equations were derived from the dynamical model shown in Figure 3. The model was used to analyze dislocation and angular deviation of the center of gravity of the elevation component when an external force  $F_e$  works on it. In this paper the external force is due to the rifle firing.

Parameter values of the vehicle platform and azimuth mechanism were obtained from the mobile robot in the laboratory at Research Centre for Electrical Power and Mechatronics, Indonesian Institute of Sciences. Spring and damping rubber were used for vibration absorber in the rifle mounting as shown in Figure 4. Table 2, Table 3 and Table 4 list up some important parameter values related to the elevation mechanism, azimuth mechanism, vibration damping spring and rubber.

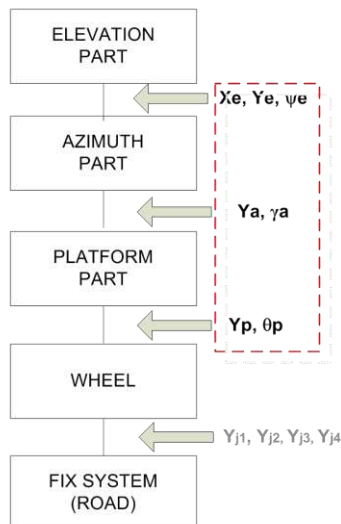


Figure 2. Weaponized vehicle structure

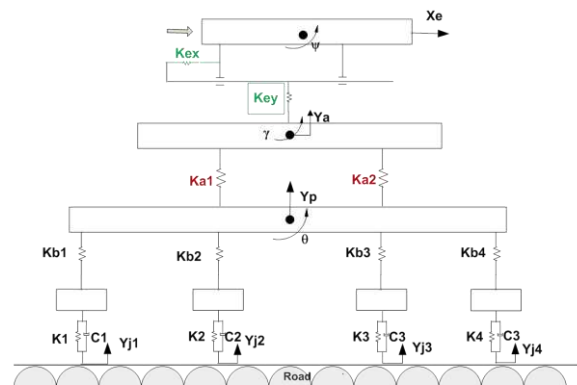
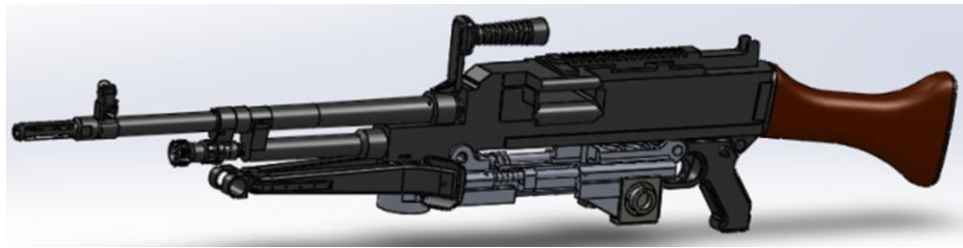
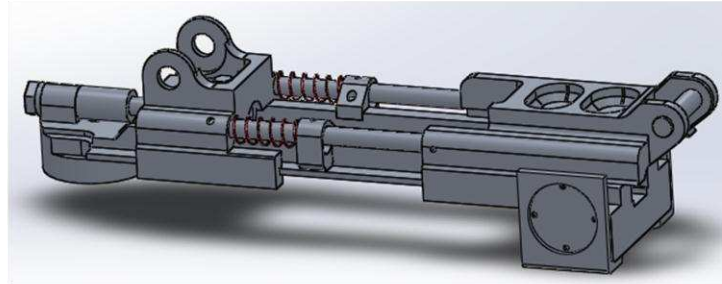


Figure 3. Armored vehicle half car model



(a)



(b)

Figure 4. Vibration absorber in the rifle mounting; (a) The rifle mounted on the elevation element; (b) Rifle mounting using spring

Table 2.  
Parameters of the azimuth and elevation components

Symbol	Description	Values
$m_a$	Azimuth weight	8.08 kg
$m_e$	Elevation weight	14.4 kg
$I_a$	Moment of inertia of azimuth component	0.412 kg.m <sup>2</sup>
$I_e$	Moment of inertia of Elevation component	1.25 kg.m <sup>2</sup>
$k_{a1}$	Stiffness coefficient at the first bushing of the azimuth component	$9 \times 10^4$ N/m
$k_{a2}$	Stiffness coefficient at the second bushing of the azimuth component	$9 \times 10^4$ N/m
$e_y$	Vertical distance between the trunion and the axis of the shoot	0.0325 m

Table 3.  
Parameter values of the spring [11, 12].

Type	Material	Stiffness(N/m <sup>2</sup> )
$k_A$	Carbon steel	$5.55 \times 10^6$
$k_B$	Stainless steel	$4.77 \times 10^6$
$k_C$	Monel Metal	$2.99 \times 10^6$
$k_D$	Brass	$2.38 \times 10^6$

Table 4.  
Parameter values of damping rubber [13, 14]

Rubber hardness	Stiffness (N/m)	Damping (Ns/m)
1. Soft	149,986.61	114.59
2. Medium	244,605.26	144.48
3. Hard	980,356.04	107.37

The rifle utilizes military bullet whose caliber is 5.56 mm x 45 mm. It can be used in three modes of firing i.e. single, semi automatic and automatic firing. In single firing mode, the shock force is 831 N which corresponds to the shock torque of 27 Nm. The shock force and torque of both semi automatic and automatic firing modes can be calculated based on the geometry and location of the rifle mounting.

The methodology is wrapped up in a flow chart illustrated in Figure 5.

- 1) Motion equation derivation of the half car model in Figure 3.
- 2) Parameter values setting based on values in Table 2 to Table 4.
- 3) Numerical parameters setting of the fourth order Runge Kutta according to Table 1.
- 4) Numerical simulation using Matlab® application software. Sampling time was set to 1 milli second.

### III. RESULTS AND DISCUSSION

First, single fire mode was applied when only spring in Table 2 was fixed in the rifle mounting. Every type of the spring effect was investigated by changing one type after another. There exists four types of spring. During every simulation, three variables were recorded, namely: horizontal dislocation (mm), vertical dislocation (mm) and angular deviation (mrad) of the center of gravity of the elevation component. With the same configuration, simulation was conducted for semi-automatic mode and automatic mode rifle firing.

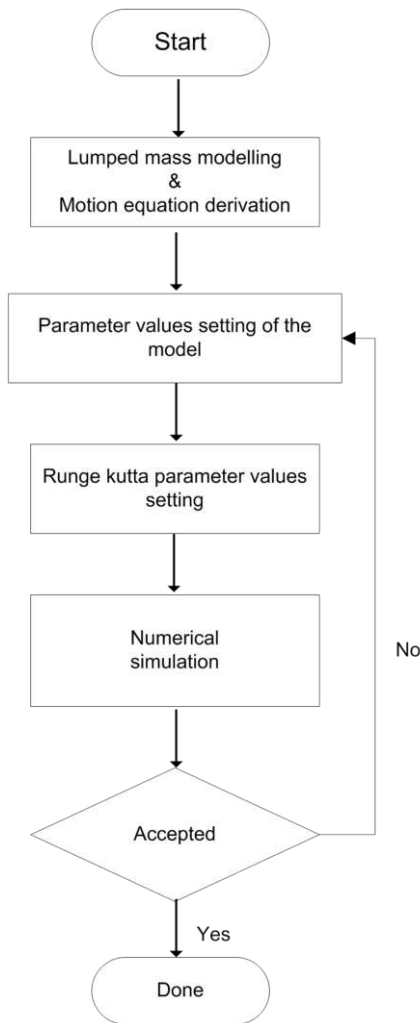


Figure 5. Calculation flow chart

Second, single fire mode was applied when only damping rubber in Table 3 was fixed in the rifle mounting. Every type of the damping rubber effect was investigated by changing one type after another. There exists three types of damping rubber. In the same way, during every simulation, three variables were recorded namely: horizontal dislocation (mm), vertical dislocation (mm) and angular deviation (mrad) of the center of gravity of the elevation component. With the same configuration, simulation was conducted for semi-automatic mode and automatic mode rifle firing.

Next, all possible combinations of serial and parallel configurations between spring and damping rubber were tested for single firing mode, semi automatic firing mode and automatic firing mode. Figure 6 shows simulation results of single firing mode when only the spring was mounted. Horizontal dislocation, vertical dislocation and angular deviation of the elevation element were plotted with time.

Figure 7 shows simulation results of single firing mode when only the rubber is mounted. Horizontal dislocation, vertical dislocation and

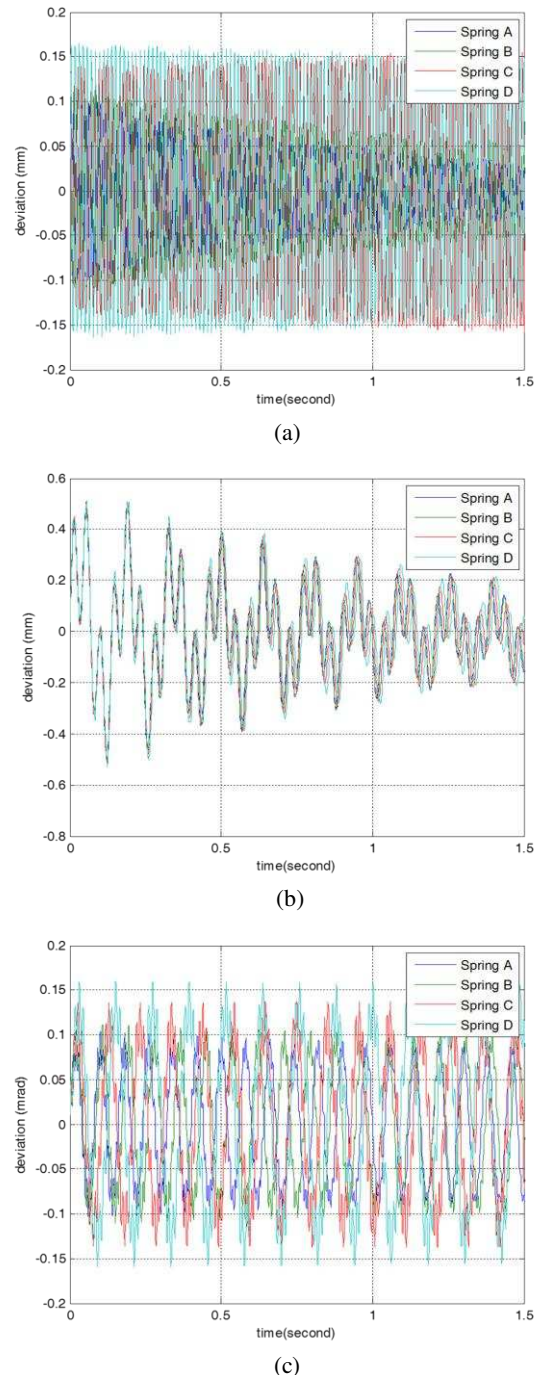


Figure 6. Single firing mode (spring only); (a) Horizontal dislocation; (b) Vertical dislocation; (c) Angular deviation

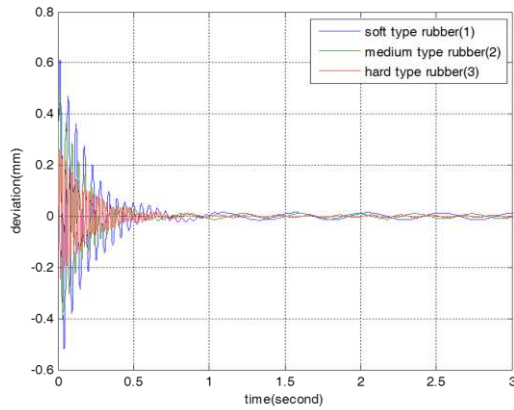
angular deviation of the elevation element were plotted with time. Figure 8 shows shock force which was generated during semi automatic firing mode. The rifle was fired three times in 0.9 second. Figure 9 shows simulation results of semi automatic firing mode when only spring was mounted.

Figure 10 shows simulation results of single firing mode when damping rubber type 3 was combined with spring in parallel configuration. Horizontal dislocation, vertical dislocation and angular deviation of the elevation element were plotted with time. Figure 11 shows simulation

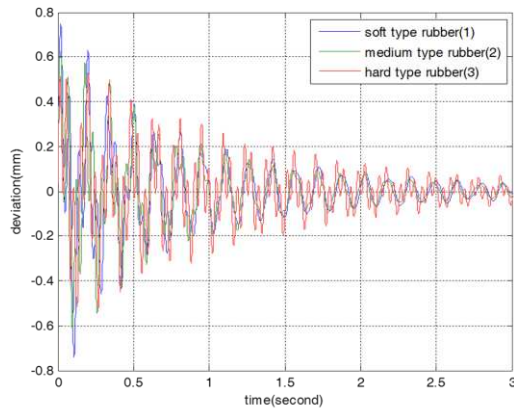


results of semi automatic firing mode when damping rubber type 3 was combined with spring in parallel configuration. Simulation of automatic firing mode was conducted by firing the rifle 12 times in 0.9 second. Its simulation results are similar to those of semi automatic ones.

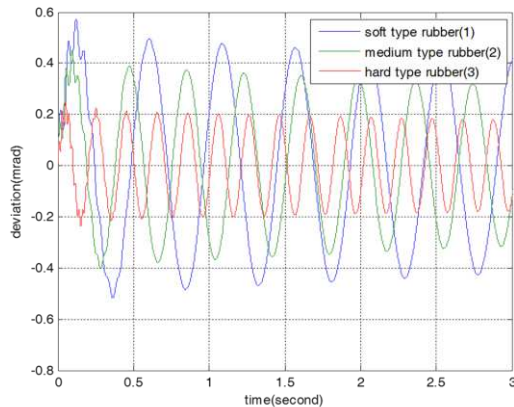
Performance of single firing mode can be analyzed using simulation results shown in Figures 6, 7 and 10. From Figure 6 it can be observed that the spring of type A produces the smallest values of angular deviation (0.104 mrad), vertical dislocation (0.506 mm) and



(a)



(b)



(c)

Figure 7. Single firing mode (rubber only); (a) Horizontal dislocation; (b) Vertical dislocation; (c) Angular deviation

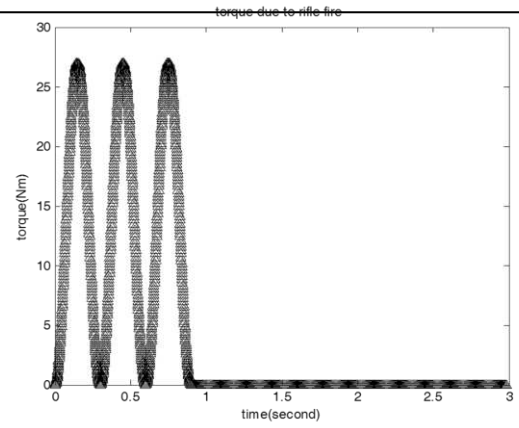
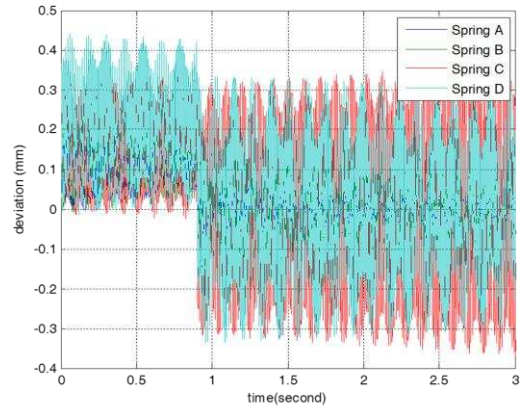
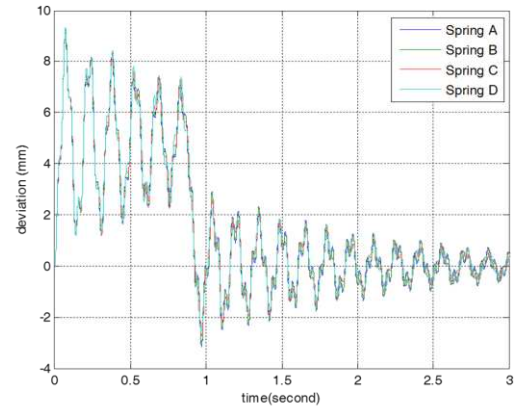


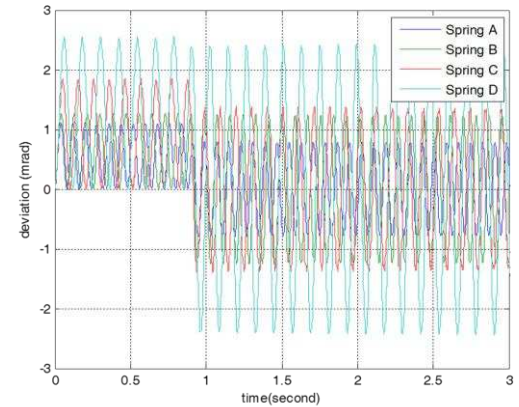
Figure 8. Rifle shock force in semi-automatic firing mode



(a)



(b)

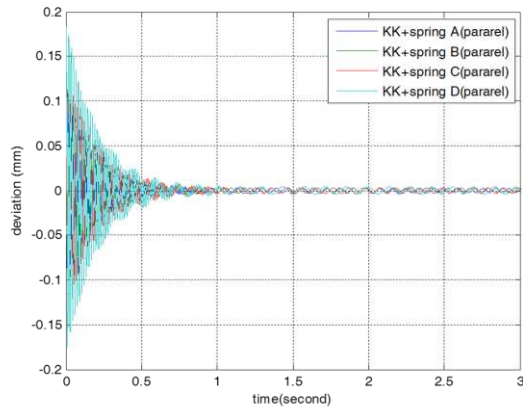


(c)

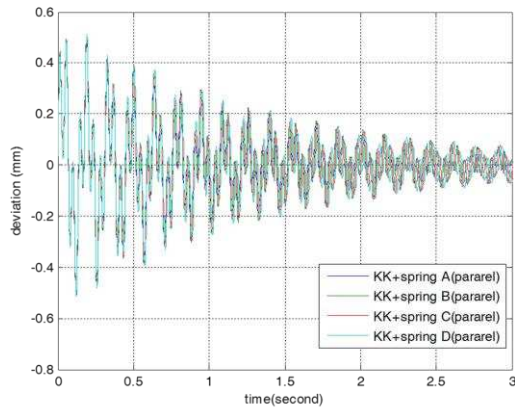
Figure 9. Semi automatic firing mode (spring only); (a) Horizontal dislocation; (b) Vertical dislocation; (c) Angular deviation

horizontal dislocation (0.104 mm). From Figure 10 it can be noted that the parallel configuration of type A spring and type 3 rubber resulted in relatively small value of angular deviation (0.11 mrad), vertical dislocation (0.507 mm) and horizontal dislocation (0.112 mm). Furthermore, this configuration performs vibration damping effect. However the damping effect in angular deviation is smaller than that in horizontal dislocation.

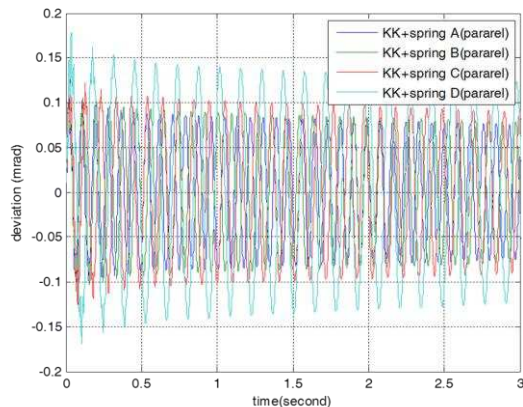
Performance of semi automatic firing mode can be analyzed using simulation result shown in



(a)



(b)

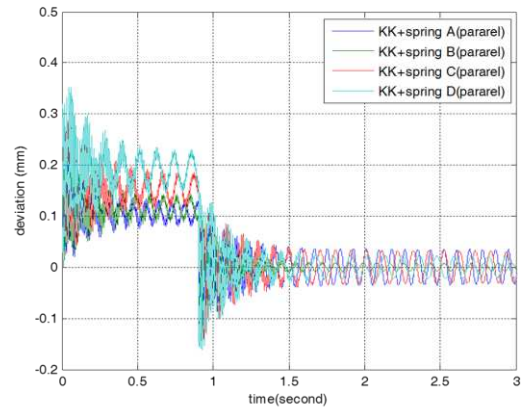


(c)

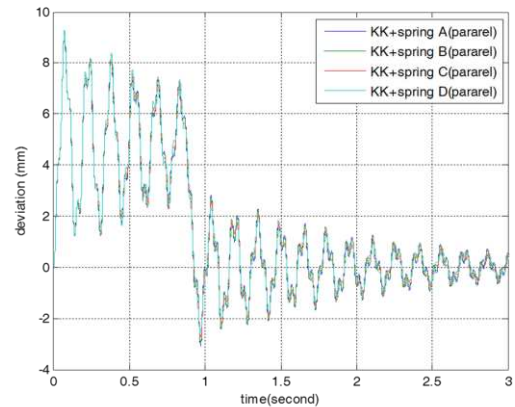
Figure 10. Single firing mode with damping rubber type 3 and spring in parallel; (a) Horizontal dislocation; (b) Vertical dislocation; (c) Angular deviation

Figure 9 and Figure 11. From Figure 9, we know that the spring of type A exhibits the smallest values of angular deviation (1.103 mrad), vertical dislocation (9.127 mm) and horizontal dislocation (0.19 mm). From Figure 11 it is obvious that the parallel configuration of type A spring and type 3 rubber provides relatively small values of angular deviation (1.26 mrad), vertical dislocation (9.15 mm) and horizontal dislocation (0.2 mm).

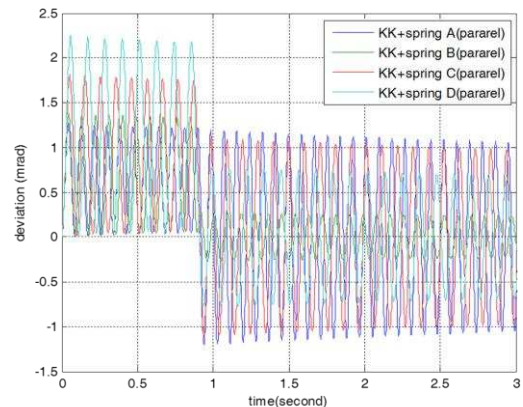
Further analysis has been done to observe effect of spring and rubber configuration on



(a)



(b)



(c)

Figure 11. Semi automatic mode with damping rubber type 3 and spring in parallel; (a) Horizontal dislocation; (b) Vertical dislocation; (c) Angular deviation

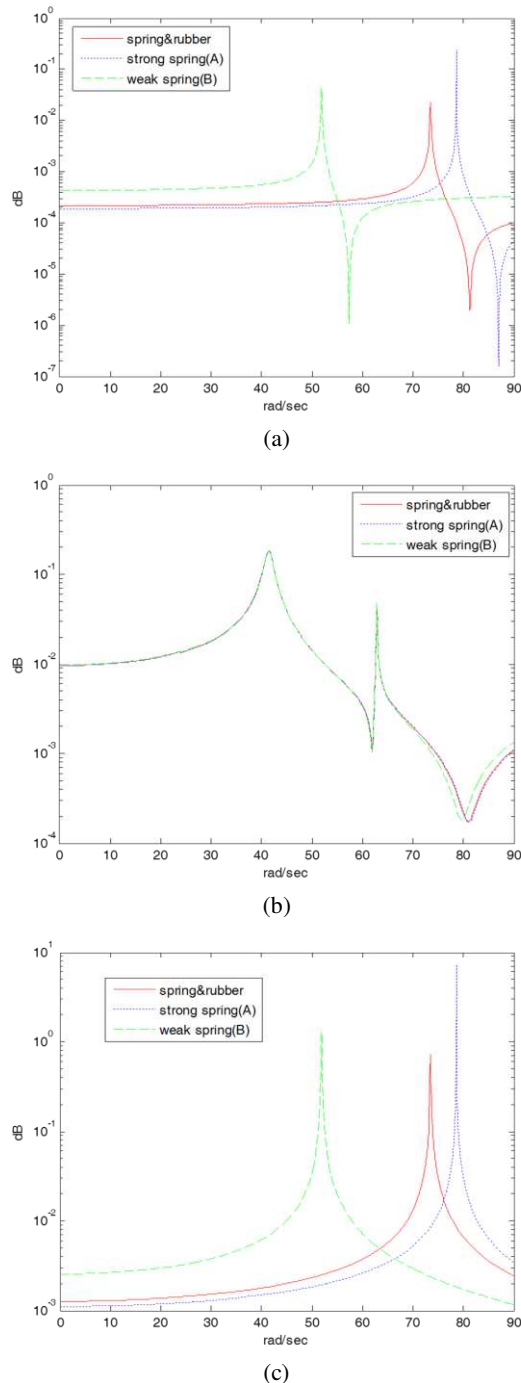


Figure 12. Bode diagram of vibration of firing arm; (a) Horizontal displacement; (b) Vertical displacement; (c) Angular displacement

displacement. Figure 12 shows Bode diagrams when using weak spring, the strong spring and the parallel configuration between damping rubber type 3 and spring A. It can be seen that the magnitude of each displacement against each parameter is different. The parallel configuration of spring A and damping rubber type 3 give the smallest peak magnitude both in horizontal displacement dan angular displacement. These results confirm the results shown in Figure 6 to Figure 11.

## IV. CONCLUSION

Parallel configuration of damping rubber type 3, with stiffness of 980,356.04 (N/m<sup>2</sup>) and damping coefficient of 107.37 (N.s/m), and Carbon steel spring with stiffness coefficient of  $5.547 \times 10^6$  (N/m<sup>2</sup>) provided the best vibration absorption. In single firing mode, angular deviation of 0.1102 mrad, vertical dislocation of 0.5065 mm and horizontal dislocation of 0.1116 mm of the elevation component were produced. In both semi automatic and automatic firing modes, angular deviation of 1.2647 mrad, vertical dislocation of 9.1516 mm and horizontal dislocation of 0.2052 mm were produced.

## ACKNOWLEDGEMENT

The authors would like to thank the Indonesian Institute of Sciences, Institut Teknologi Bandung, and Indonesian Ministry of Research and Technology for the opportunity and financial support in conducting this research.

## REFERENCES

- [1] F. Schillebeeckx, J. Peirs, V. W. Vijver, D. Reynaerts, "Compact zero-backlash tilt-pan mechanism based on differential gear technology," 9<sup>th</sup> International Conference on New Actuators, pp. 641-644, 2004.
- [2] W. E. Dixon, D. M. Dawson, E. Zergeroglu Malithong, "Adaptive tracking control of a wheeled mobile robot via an uncalibrated camera system," IEEE Transactions on Systems, Man, and Cybernetics, Vol. 31, pp.341-352, 2001.
- [3] H. M. Saputra, Z. Abidin, E. Rijanto, "IMU Application in Measurement of vehicle position and orientation for controlling a pan tilt mechanism," Journal of Mechatronics, Electrical Power, and Vehicular Technology, 2013, Vol.4, No.1, pp.41-50. doi:10.14203/j.mev.2013.v4.41-50.
- [4] M. Mirdanies, A. S. Prihatmanto, E. Rijanto, "Object recognition system in remote controlled weapon station using SIFT and SURF methods," Journal of Mechatronics, Electrical Power, and Vehicular Technology, 2013, Vol.4, No.2, pp.99-208. doi:10.14203/j.mev.2013.v4.99-108
- [5] R. P. Saputra, E. Rijanto, H. M. Saputra. 2012. "Trajectory scenario control for the remotely operated mobile robot LIPI platform based on energy consumption

- analysis,” International Journal of Applied Engineering Research, Vol.7, No.8, pp.851-866.
- [6] E. Rijanto, R. P. Saputra, H. M. Saputra. 2013. “Positioning control for the mobile robot LIPI articulated robot arm based on PD control approach,” International Journal of Applied Engineering Research, Vol.8, No.4, pp.423-433
- [7] J. Balla, “Dynamics of mounted automatic cannon on track vehicle,” International Journal of Mathematical Models and Methods in Applied Sciences., Vol.5, pp.423-432, 2011.
- [8] J. Biti, “An Investigation of damping supercar,” Bachelor of Engineering, School of Mechanical and Manufacture Engineering, 2008.
- [9] D. C. Akiwate, S. S. Gawade, “Design and performance analysis of smart fluid damper for gun recoil system,” International Journal of Advanced Mechanical Engineering, Vol. 4, No. 5, pp. 543-550, 2014.
- [10] W. Borkowski, P. Rybak, Z. Hryciów, J. Wysocki, K. Papliński, B. Michałowski., “Operational loads of combat vehicles,” Journal of KONES Powertrain and Transport, Vol. 18, No. 1, 2011.
- [11] E. H. Choi, J. B. Ryoo, J. R. Cho, O. K. Lim, “Optimum suspension unit design for enhancing the mobility of wheeled armored vehicles,” Journal of Mechanical Science and Technology, Vol. 24, pp. 323-330, 2010.
- [12] S. Sulaiman, P. M. Samin, H. Jamaluddin, R. A. Rahman, M. S. Burhaumudin, “Groundhook control of semi-active suspension for heavy vehicle,” International Journal of Research in Engineering and Technology (IJRET), Vol. 1, No. 3, pp.146-152, 2012.
- [13] A. C. Mitra, N. Benerjee, “Vehicle dynamics for improvement of ride comfort using a half car bondgraph model,” International Journal of Researchers, Scientist and Developers., Vol 2, 1-5, 2014.
- [14] O. Bayrakdar, “Random vibration of road vehicle,” Master Thesis, Master of Science, Izmir Institute of Technology, 2010.
- [15] Schmid, Hamrock, Jacobson, *Fundamentals of machine elements*, 3<sup>rd</sup>, CRC Press, 2014.
- [16] G. Stigliana, D. Mundo, S. Donders, T. Tamarozzi, “Advanced vehicle body contact modelling approach using reduced models of beams and joint,” in Proceedings of Isma, pp. 4179-4190, 2010.
- [17] F. L. Neto, B. Santos, “A Procedure for the parametric identification of viscoelastic dampers accounting for preload,” J. of the Braz. Soc. of Mech. Sci. & Eng., Vol.XXXIV, pp. 213-218, 2011.
- [18] A. Shirahatt, P. Prasad, P. Panzade, M. Kulkarni, “Optimal design of passenger car suspension for ride and road holding,” Journal of the Brazilian Society of Mechanical Science and Engineering, Vol.XXX, pp. 66-76, 2008.
- [19] M. Bayat, I. Pakar, “On the approximate analytical solution to non-linear oscillation systems,” Journal of Shock and Vibration, Vol. 20, pp. 43-52, 2013.
- [20] H. Yaghoobi, M. Torabi, “An analytical approach to large amplitude vibration and post-buckling of functionally graded beams rest on non-linear elastic foundation,” Journal of Theoretical and Applied Mechanics, pp. 39-52, 2013.
- [21] T. Salau, K. A. Olaiya, O. O. Ajide, “Simulation of oscillators dynamics using selected versions of fourth order runge-kutta scheme,” International Journal of Engineering and Technology Vol.4 No. 8, pp. 444-450, 2014